5

Optimization of composite forming

W-R YU, Seoul National University, Korea

5.1 Introduction

This chapter is concerned with the optimization of composite forming, especially sheet forming, a manufacturing process that transforms a flat sheet of composite or preform into a three-dimensional shape. Over the last decade, the process of automated sheet forming for composites has emerged from the metal forming process, making use of existing science and technology, and has overcome a prolonged manufacturing process for composites. In the design of the forming process it is vital to predict the deformation behavior of composite sheets, since this helps to prevent defects that can develop as a result of forming tools interacting with the composite materials. Numerous studies have been carried out to develop mechanics models (e.g., Yu, 2002, 2005) that simulate the deformation behavior of composite sheets, and to combine these simulations to analyze the forming behavior of composite sheets. Such models aim to optimize the forming process for manufacturing composite parts with the minimum of defects.

This chapter provides the reader with an overview of the current state of composite forming optimization studies. Optimization methodology in itself is a well documented topic (Luenberger, 1989) and has been applied to many fields ranging from product design and performance to manufacturing processes. In general, the optimization of composite forming includes a cost analysis for materials, energy, tooling and machinery, and a performance analysis, based on variables such as high strength and stiffness considering the minimum weight and thickness of the product. However, this chapter focuses on the optimization of process parameters which can form composite sheets into complex three-dimensional parts with no, or minimal defects. In addition, since many processes are frequently too time consuming or too expensive for optimization based on physical experimentation, researchers have increasingly relied on mathematical models to simulate these processes. Advances in computational power have enabled more extensive use of such models. Therefore, the current chapter discusses optimization of composite forming using models that rely on computational experiments.

Since the literature on optimization studies of composite forming is still limited compared to other manufacturing fields such as sheet metal forming, this chapter discusses optimization strategies adopted in sheet metal forming, which may be a good starting point for analyzing optimization strategies for composite forming. In Section 5.2, general aspects of optimization methods are discussed briefly to help the reader understand the mathematical aspect of optimization methodology and identify the limitations of directly applying well-known methods of optimization, such as the downhill simplex and conjugate gradient method, to computational simulation experiments. Section 5.3 discusses objective functions for the optimization of composite forming and the methodological basis for this.

5.2 General aspects of optimization

5.2.1 Optimization methods

This subsection describes the mathematical aspects of optimization methodologies in order to set the basis for the subsequent discussion in this chapter. A thorough explanation of these methods can be found in many text books (Luenberger, 1989; Press, 1992).

The first step in any optimization process is to determine an objective function f that depends on one or more independent variables. The objective function can represent any quantities pertinent to the relevant process, such as manufacturing expenditure, cost and duration, physical properties such as weight and thickness, mechanical performance variables such as strength and modulus, and qualities of the formed product such as wrinkling and defects. The optimization task involves obtaining suitable values for the independent variables where the value of f is maximized or minimized. The tasks of maximization and minimization involve the same process, since the minimization of function f is equal to maximization of $-f$. The objective function can be expressed in an analytic form, although in practice it is often comprised of discrete data which necessitates transformation of the data into a function of independent variables using a regression model. The objective function is very often assumed to be an unknown black box scenario with independent input variables.

After the objective function is defined, the optimization procedure expedites the search for independent variables sets where the objective function has a minimum value. Many algorithms for effective searches have been developed. These algorithms are categorized into two methodologies; first those that rely on function value only, such as the downhill simplex (DS) method; and secondly those that rely on such additional information as the gradient of the objective function, as is the case with the conjugate gradient (CG) method. There follows a brief discussion of the two methods (DS and CG) to understand the iterative

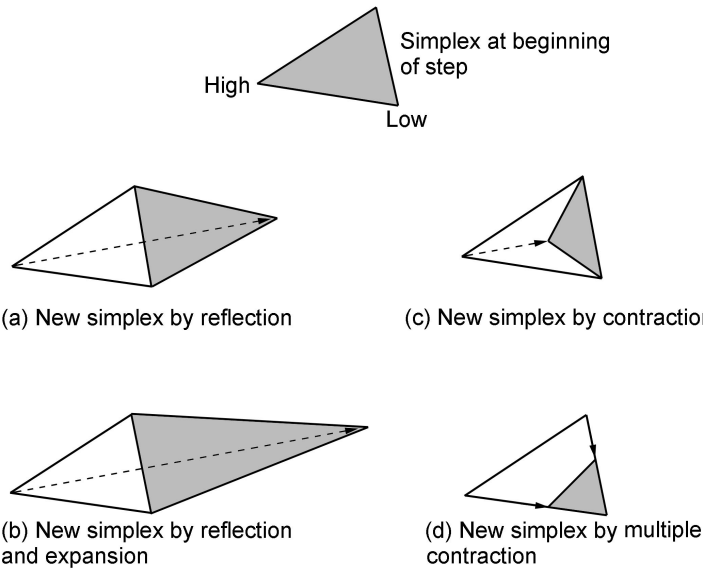

5.1 Possible outcomes for a step in the downhill simplex method.

nature of optimization as well as to help to choose a proper method for process optimization using computational experiments.

Since the DS method requires function evaluation only without derivative information, it may be not very efficient in a number of the function evaluations. However, the DS method is frequently used in optimization procedures because it directly searches for the minimum value of the objective function. A 'simplex' is a geometrical figure consisting, in N dimensions, of N+1 points and all their interconnecting line segments (polygonal faces). In two dimensions, a simplex is a triangle. The search process is described by the successive formation of a new triangle. The search algorithm starts with the function evaluation of any three design points. It is natural to move the highest point in the triangle to another one when searching for the minimum value of a function. The algorithm for the new triangle can be built in numerous ways, although four strategies in particular are usually adopted, and these are shown in Fig. 5.1 (Press, 1992). Visualization of the search process for an analytical function is helpful clearly to understand an optimization scheme. The Rosenbrock function is chosen for the purposes of this discussion.

The Rosenbrock function is characterized by one long curved valley as given in Equation (5.1). See Fig. 5.2 for the mesh and contour plot for the two-dimensional case (i.e., $n = 2$).

$$f(x) = \sum_{n=1}^{n-1} \left(100(x_{i+1} - x_i^2)^2 + (x_i)^2 \right) \qquad 5.1$$

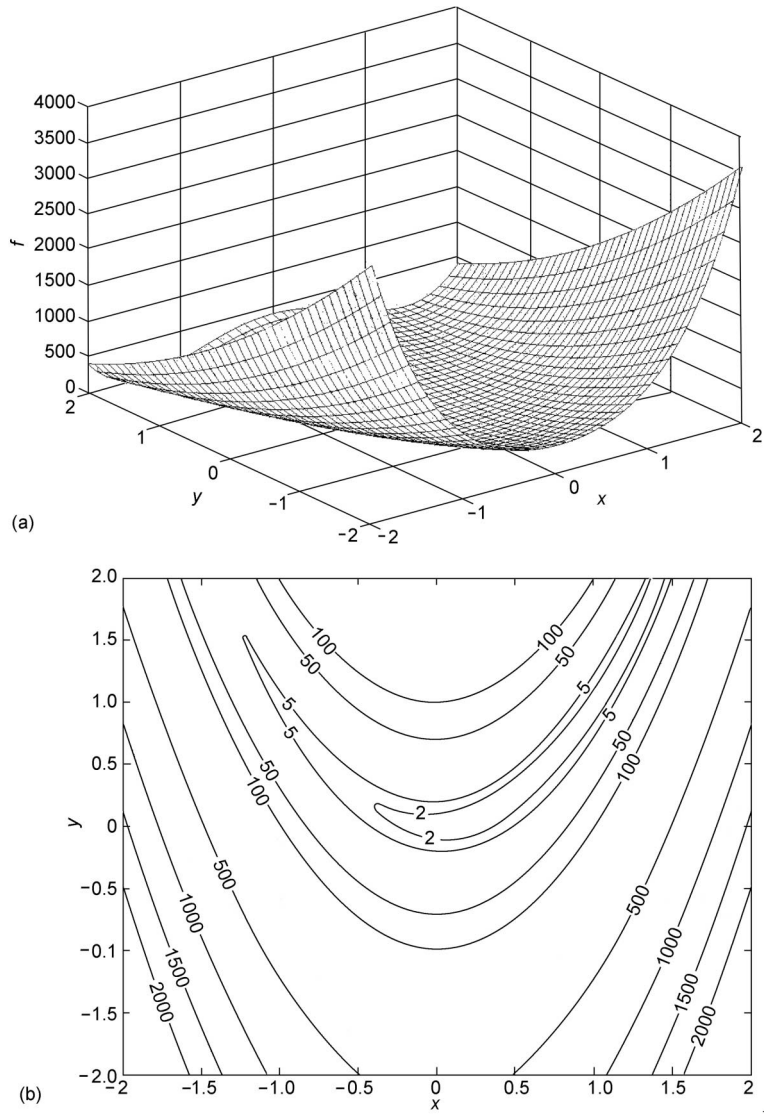

5.2 Rosenbrock functions in two dimensions.

Implementation of the DS method provides the basic knowledge for optimization. The details for computer implementation can be found in many text books (e.g., Press, 1992) and optimization (or minimization) results for the Rosenbrock function are shown in Fig. 5.3. Convergence speed is an important feature for evaluating the performance of an optimization method since slow convergence may indicate that the optimization method requires more function evaluations than other methods, thereby increasing the costs of the optimization procedure.

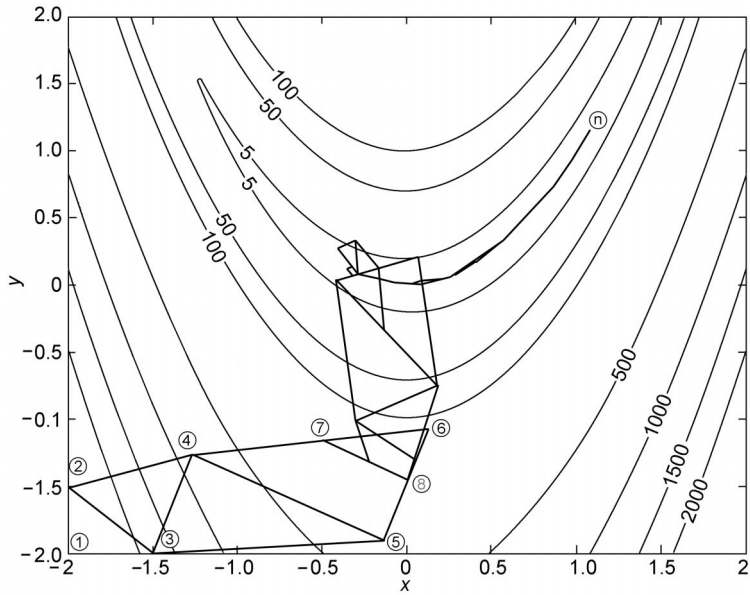

5.3 Implementation of DS for minimizing Rosenbrock function. The optimum (minimum) point is (1,1). Number 4 in the circle is constructed by reflecting number 1, and by forming a new simplex consisting of 2, 3, and 4 points. Numbers 5 and 6 are also generated by reflecting and expansion, while numbers 7 and 8 are searched by multiple contraction, and so on.

As shown in Fig. 5.4, the convergence speed of the DS method is very slow, implying that the method may not be cost-effective.

For process optimization procedures that use computational experiments, it is important to reduce the number of simulations because a single simulation may need a computation time of the order of hours, or sometimes even days, on a modern workstation. Furthermore, parallel simulations, which enable different sets of process parameters to be evaluated on separate computers simultaneously, can be incorporated into optimization schemes to reduce the actual time for performing the optimization procedure. In this regard, the first N+1 points for the first simplex can be obtained using parallel simulation, but the successive points for the new simplex are dependent on the previous results, and cannot benefit from parallel simulation as a result. There are two ways of reducing the computation time of process optimization; one way is to actually reduce the number of simulations, as is the case with the conjugated gradient (CG) method; another way is to utilize parallel simulations that are performed on a clustered computer system.

The conjugated gradient (CG) method requires not just the value of the objective function $f(\mathbf{P})$ at a given N-dimensional point $\mathbf{P}$, but also the gradient $\nabla f(\mathbf{P})$. The CG method consists of setting up a direction on which the

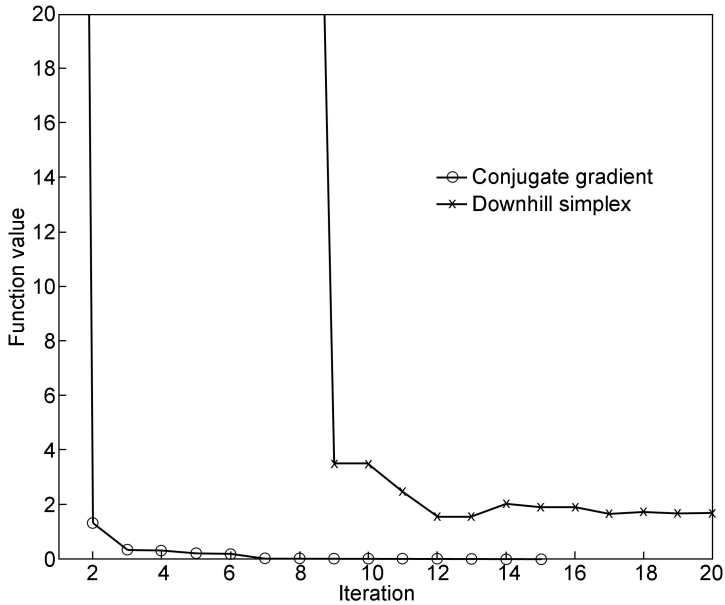

5.4 Convergence of downhill simplex(DS) and conjugate gradient (CG) for the Rosenbrock function in the two dimensional case.

minimization process is performed using a line search. For such directions, a coordinate axis, such as, for example, (1,0) and (0,1) in a two-dimensional case, can be chosen. However, successive minimization along coordinate directions is known to be extremely inefficient since it can take many steps to get to the minimum value through repeated crossing and re-crossing of coordinate directions. To avoid the crossing and re-crossing of a direction, the GC method mathematically defines a 'non-interfering' direction (the so called 'conjugate direction'), along which the minimization process is not spoiled by subsequent minimization along another direction.

Suppose that a movement takes place along some direction $\mathbf{u}$ to a minimum, and it is now proposed to move along a new direction $\mathbf{v}$. The condition that a motion along direction $\mathbf{v}$ does not spoil the minimization along direction $\mathbf{u}$ may be that the gradient at the previous minimum point in direction $\mathbf{u}$ stays perpendicular to $\mathbf{u}$ because the gradient determines the new direction to be searched. This condition can be mathematically expressed, with $\mathbf{x}_1$ and $\mathbf{x}_2$ being design points (parameter sets) on the direction $\mathbf{v}$:

$$\nabla f(\mathbf{x}_1) \cdot \mathbf{u} = 0, \nabla f(\mathbf{x}_2) \cdot \mathbf{u} = 0 \tag{5.2}$$

$$(\nabla f(\mathbf{x}_2) - \nabla f(\mathbf{x}_1)) \cdot \mathbf{u} = \delta(\nabla f) \cdot \mathbf{u} = 0 \tag{5.3}$$

Here, the variation of the gradient may be approximated by the following Equation (5.4):

$$\delta(\nabla f) = \frac{\partial^2 f}{\partial x_i \partial x_j}\delta x_j \mathbf{e}_i = \mathbf{A}\cdot\mathbf{v} \tag{5.4}$$

Finally, the 'non-interfering' condition can be written as the following Equation (5.5):

$$\mathbf{u}\cdot\mathbf{A}\cdot\mathbf{v} = 0 \tag{5.5}$$

When Equation (5.5) holds for two vectors **u** and **v**, it can be said to be conjugate. Therefore, conjugate gradient methods consist of first determining successive conjugate directions and then performing a one-dimensional minimization process along the conjugate direction. For one-dimensional minimization (line search), the 'Golden section method' and 'Brent's method' without or with information of the first derivative of function are frequently used. Furthermore, since the conjugate direction can be evaluated using the first derivative of function (i.e., gradient $\nabla f(\mathbf{x})$) without calculating the second derivative of function as in Equation (5.4) (Luenberger, 1989), this optimization method is called the conjugate 'gradient' method. The searching process of CG method along a new conjugate direction is illustrated in Fig. 5.5 for the two-dimensional Rosenbrock function. As demonstrated in Fig. 5.4, the CG method

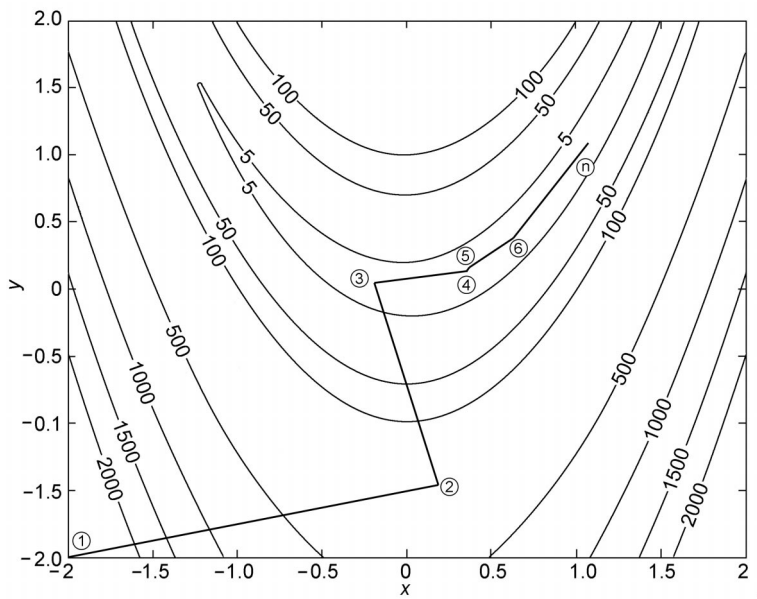

5.5 Implementation of CG method for minimizing a two-dimensional Rosenbrock function. The optimum (minimum) point for the function is (1,1). The first step is to set a conjugate direction on which minimization (line minimization) is performed to generate the number 2. The second conjugate direction at the number 2 is also determined and line minimization along the direction is performed. This procedure continues until successive points get to the minimum point.

is a more effective optimization method than the DS method since it requires a smaller number of function evaluations.

When the CG method is applied to optimization problems using computational experiments, parallel simulations need to be utilized to reduce the optimization time. When determining new conjugate directions, the CG method needs the gradient of function which can be calculated using parallel simulations. In addition, line minimization can be performed based on function evaluations that are provided using parallel simulations. Though a parallel simulation scheme may be incorporated, CG methods may need many numbers of iterations for successive searches, thereby increasing the optimization time. A surrogate model can be used as an optimizer in order to benefit from parallel simulations using computer modeling techniques. This is discussed below.

5.2.2 Optimization using a surrogate model

Process optimization can be performed using a surrogate model (Jakumeit, 2005; Chengzhi, 2005). The surrogate model is referred to an approximate model fitting sample data. In this optimization strategy, the first step is to determine the parameter sets, **X** (design points), for which the simulation is performed. In the second step, the objective value $f(\mathbf{X})$ at the design points is used to build a surrogate model as an approximation to the actual data. The third step is to search for the minimum (or optimum) function of the surrogate model. Since the surrogate model approximating sample data is an analytic function, the third step of minimization can be performed quickly using the DS or CG method discussed in Section 5.2.1. If the new optimum is close to the last optimum (convergence) and if the estimate of the surrogate model is close to the results obtained by following a complete simulation, the algorithm then stops, the assumption being that the minimum point has been reached. Otherwise, the surrogate model is improved in a further iteration by adding additional simulations at the new points or by reducing the modeled region. This approach has an advantage over the DS or CG method in that it can maximize the benefit of the parallel simulations.

The responsive surface method (RSM) is a common method of building a surrogate model (an approximate model) in which a polynomial function of varying order (usually a quadratic function) is fitted to sample data using a technique of least square regression (Myers, 2002). It can provide an explicit functional representation of the sampled data which is obtained experimentally or computationally. However, RSM has several limitations. It is unable to predict multiple extrema. In addition, RSM was originally developed to model data obtained from physical experiments which had a random error distribution. Since computational experimentation is a deterministic process (the input produces the same result), in statistical terminology random errors are not present in computational experiments; RSM may not be a proper model

for approximating deterministic (computational) data (Sacks, 1989). Researchers have developed the Kriging method to overcome this limitation (Sacks, 1989).

The Kriging method is very similar to RSM but provides an interpolation modeling technique to approximate the results of the deterministic computational experiments. It consists of the sum of many local functions (frequently the Gauss function) and one global function, which may be a polynomial as in RSM. The local function is used to bridge the difference between the global function and the simulation results using a maximum likelihood estimate, which allows for capturing multiple local extrema. A more detailed description of the Kriging method can be found in the work of Sacks (1989). The implementation of the Kriging method can be carried out using the Matlab Kriging Toolbox which is open to the public (Lophaven, 2002).

Figure 5.6 shows the response surface for a two-dimensional Rosenbrock function, which was constructed using the Kriging method. The optimization is now performed easily on the response surface that is analytically expressed, so that any minimization algorithm (DS or CG method) can be utilized. Here, a couple of issues arise when considering the Kriging response surface as an optimizer. The first issue concerns the number of design points (parameter sets), an issue is directly related to the number of simulations. Simply stated, the answer may be 'the more the better' since interpolation in the surrogate model is improved as the volume of data increases. However, it is not possible to increase the volume of data infinitely. Thus, a proper number of design points should be set up for the first time (e.g., eight points) which can be determined by the

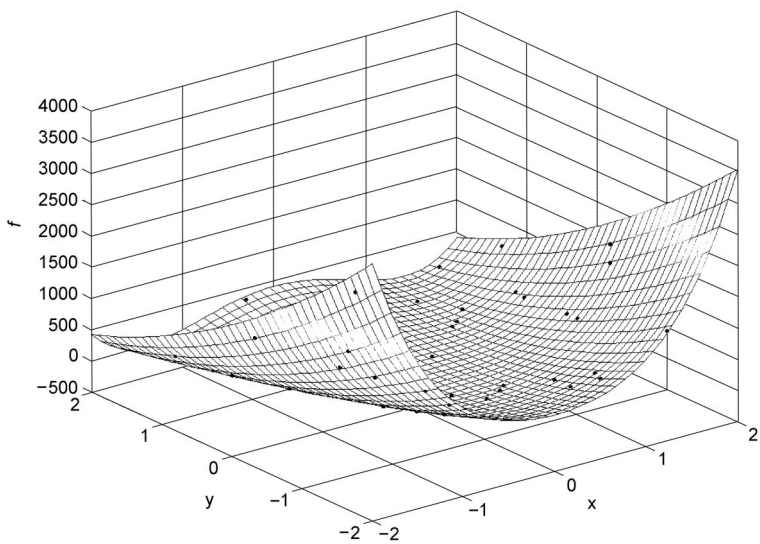

5.6 Response surface constructed using Kriging method for the two-dimensional Rosenbrock function.

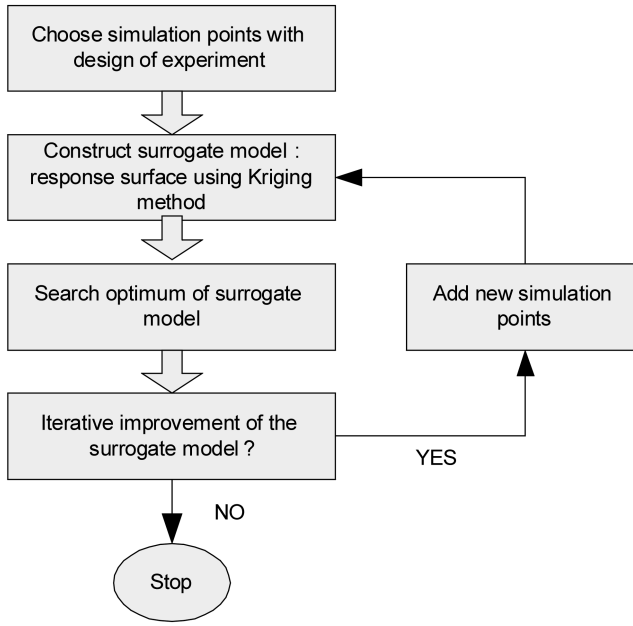

5.7 Flowchart of an optimization strategy using surrogate models.

parallel simulation capability. The optimization is then performed on the surface that was constructed based on the first design points. If the result is not good enough, the surrogate model can be improved by adding new design points with which a new simulation can then be done. Such addition of new design points can continue until it is no longer necessary to improve the response surface. Such an algorithm is depicted in Fig. 5.7. Conceptually, this algorithm is not difficult to understand for implementation. However, many algorithms exist in practice and this indicates that a solid strategy for moving the design boundary and for adding new design points during optimization should be established for its wide application to composite forming.

5.3 Optimization of composite forming

This section describes objective functions and actual optimization methods for composite forming. The first step in optimization study is to identify the objective function. In general, several different objectives may compete with each other, such as, for example, the manufacturing time and cost, and the quality or performance of a formed product. Section 5.3.1 discusses objective functions and provides a brief explanation of the composite forming process. The section then focuses on the process optimization of composite forming, including preform shape and the blank holding force (BHF).

5.3.1 Objective functions in composite forming

In composite forming, various processing parameters are pertinent to the forming process. For thermoplastic and thermoset prepreg forming, the relevant parameters can be classified as heat related, external force related, and material shape related parameters. In the preform forming, heat related factors are not relevant. As thermoforming methods for thermoplastic prepreg, the diaphragm (Delaloye, 1995) and stamp forming (Hou, 1994) processes are well known. Both forming processes consist of three stages; first the stage of heating thermoplastic prepreg to a temperature for matrix flow, secondly the stage of shaping and consolidating heated and flat prepreg into complex and curved parts, and finally the cooling stage. As such, the thermoforming process needs significant processing time for all the three stages, so that the first objective of the thermoforming process may be to reduce the cycle time. Since the majority of process time is related to the heating of prepreg, an objective for process optimization may be to pursue a suitable heating method that can elevate the temperature of prepreg as rapidly as possible. This optimization problem can be solved by developing a heating unit that uses convection, conduction, or infrared or a combination of these methods. Therefore, this optimization may be purely related to the development of a mechanical heating unit.

The last stage of the thermoforming process, which will be discussed briefly before the second stage of thermoforming is discussed in some detail, is the cooling stage where two objectives compete for the optimization of the cooling process. One objective is to allow the correct molecular arrangement for the crystallization of the matrix and another is to shorten the cooling time in order to reduce the cycle time. The optimization problem at this stage can be stated as 'minimizing the cooling time while allowing the resin matrix to orient and crystallizes. The molecular movement and crystallization can be assessed as a function of the cooling time and its profile in order to solve this optimization problem.

In the second stage of thermoforming, the mechanical force by pressure (or a vacuum) in the diaphragm or of the punch in the stamp forming is applied to the heated and flat prepreg, shaping it into curved and complex parts. The fiber reinforcement, especially continuous fiber, experiences compressive stress and fibers may kink or buckle unless a mechanism is adopted that releases this compressive stress. For the release of compressive force, a resin matrix allows fibers to slip within a viscous media, and this requires that the material temperature is maintained high enough to allow matrix flow. As such, the shortening of processing time for the shaping, as well as for minimizing the heat dissipation, may be necessary. In this respect, the objective in process optimization may be 'to find a proper pressure or stamp velocity for maintaining matrix flow', and this optimization can be solved by measuring or calculating heat transfer within prepreg as a function of the stamp or pressure velocity.

Another useful method to prevent or relax compressive force is to apply tension to the prepreg during shaping. In the diaphragm forming process, the biaxial extension of the flexible diaphragm can impart tension to the prepreg, the extent of which is determined by the material properties of the diaphragm. In the stamp forming process, a blank holding force (BHF) is introduced through a blank holder, and this offers a more flexible mechanism for tension control. Therefore, the processing variable to be optimized in the shaping stages is mechanical force and its profile, the extent of which can be determined through a selection of diaphragm material or BHF.

The quality of a formed product can be characterized in terms of its thickness, uniformity, fiber orientation, and by defects such as fiber breakage and in-plane and out-of-plane buckling. The optimization problem in the shaping stage can be rephrased in terms of 'determining the processing variables (mechanical shaping force and BHF) to minimize thickness diversity, fiber orientation diversity, fiber breakage and wrinkling'. As more than one objective function is involved, the optimization of the shaping process is by nature a multi-objective optimization problem. Since the exact or analytic relationship between such objectives and process variables is difficult, or even at times impossible, to derive, the relationship is characterized as a 'black box' relationship, indicating that actual values of the objective functions are only obtained by virtual (computational) or actual experiments. Each objective function in composite forming is described below.

Thickness diversity may be expressed by, for instance, Equation (5.6) as follows:

$$H = \sum_{i=1} (h_i - \bar{h})^2 \tag{5.6}$$

where i indicates material points, and h_i and $\bar{h}$ are its thickness and the average of the thickness, respectively. The degree of fiber orientation distribution in the formed parts is expressed in Equation (5.7) as follows:

$$\Theta = \sum_{i=1} (\theta_i - \bar{\theta})^2 \tag{5.7}$$

where i represents material points, and θ_i and $\bar{\theta}$ are the fiber angle and the average fiber angle in the formed part.

The objective function for fiber breakage is described by fiber strain, providing a constraint for maximum allowable strain expressed in Equation (5.8) as follows:

$$\epsilon_f \leq \epsilon_{\max} \quad \text{or} \quad \Xi = (\epsilon_f - \epsilon_{\max}) \tag{5.8}$$

where ϵ_f and $\epsilon_{\max}$ are fiber strain in prepreg and the breaking strain of fiber respectively.

An objective function for representing wrinkling or buckling is more complex because it needs a criterion that predicts its occurrence in formed parts. Little

literature has been dedicated to developing a wrinkling criterion. For woven structures, wrinkling was reported to occur as the fiber angle approaches a specific angle (jamming angle) (Prodromou, 1997). Certainly, this may be true in that the main deformation mode in the woven reinforced prepreg or preform is intra-shearing, and the yarns may buckle out as the shear deformation is not possible due to warp and weft fiber touching each other. This is because buckling facilitates the release of build-up stresses. In this case, the objective function for wrinkling minimization may be as set out in Equation (5.9):

$$\Psi = \sum_i (\theta_i - \theta_{jam})^2, \theta_i > \theta_{jam}, \text{ otherwise } \Psi = 0 \qquad 5.9$$

where i represents material points, and θ_i and θ_{jam} are the fiber angle and the jamming angle. However, the above criterion may be not applicable to the unidirectional lamina and other knitted reinforcements. In addition, wrinkling can be observed even where the fiber angle between the warp and weft does not reach the jamming angle, implying that the jamming angle is not the only mechanism for wrinkling.

The optimization procedure can be performed by searching the minimum of those objectives. The multi-objectives set out in Equations (5.6) to (5.9) can be translated into a single objective function using the following weight factors set out in Equation (5.10):

$$f = \rho_i H + \rho_2 \Theta + \rho_3 \Xi + \rho_4 \Psi \qquad 5.10$$

where ρ_i are weight factors for each objective.

The design set of minimizing Equation (5.10) can be obtained using one of the optimization methods described in Section 5.2. Since it is not unusual that the systematic determination of the weight factors is not possible, the single objective function in Equation (5.10) may be not proper; instead, a multi-objective optimization method may be more appropriate.

It may be useful to review objective functions in other fields of forming. The quality of a formed sheet of metal is assessed by severe thinning, which may cause tearing, and by wrinkling. Since sheet metal forming involves the stretching of thin sheets, the principal strains are used to predict where such defects in a forming operation occur. Using experiments or theoretical calculations, the region in which such defects may occur can be identified in terms of principal strains, the limits of which can be expressed in a forming a limit diagram as shown in Fig. 5.8. The optimization process in this case is to 'pursue a processing path and a preform shape in order that one of the material points does not experience strains beyond the forming limit'. Mathematically, the optimization process is equivalent to the minimization of a potential representing the forming limit.

Composite forming has also adopted the technique of a similar forming limit diagram. Researchers (Tucker, 1998) have studied a forming limit diagram for

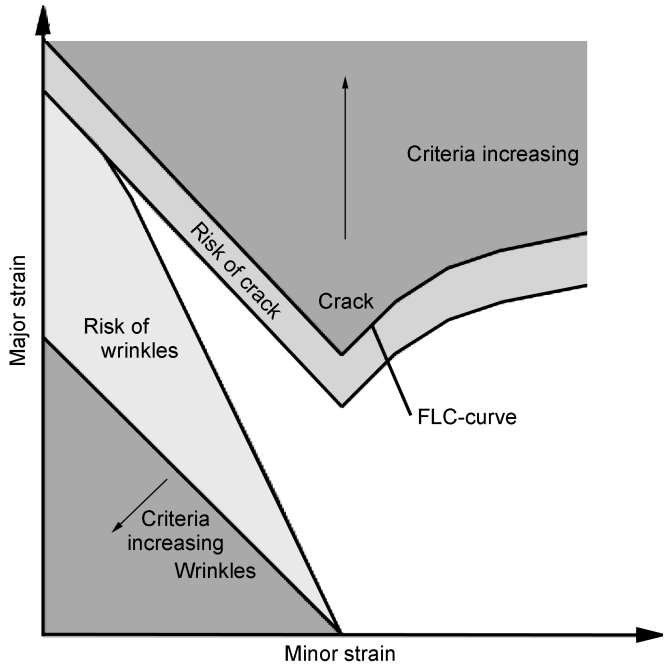

5.8 Schematic formability limit diagram for sheet metal with critical regions for crack, risk of crack, risk of wrinkles and wrinkles (Jakumeit, 2005).

the random fiber mat to develop a shape optimization method. The key premise in this forming limit diagram was that the defects of the forming random mat preform can be quantified with a limit diagram obtained by multi-state loading experiments as shown in Fig. 5.9. The forming limit diagram divides the strain space represented by principal stretches, λ_1 and λ_2, into regions where defects (wrinkle or tears) are likely to occur, and into regions of acceptable deformation without such defects. Several experiments are performed to evaluate the points U, P, and B which mark the boundaries of the acceptable regions of principal strain. Points U, P and B can be determined from a uniaxial elongation test, a pure shear test, and an equi-biaxial stretch test respectively. The boundary PB is found from unequal biaxial stretching experiments performed using various ratios of λ_1 to λ_2. More details can be found in a research paper by Tucker (2003). In this case, the optimization of the forming process can be defined as 'finding process parameters that keep the local strain at every point in the preform away from the boundaries UO and UPB'.

This section has outlined various objective functions involved in composite forming, in particular for thermoplastic composite forming. For preform forming without a resin matrix, the considerations pertinent to the first and third stages of the process are not necessary because preform forming without a resin matrix does not involve heat. Material flow or deformation is dependent on preform

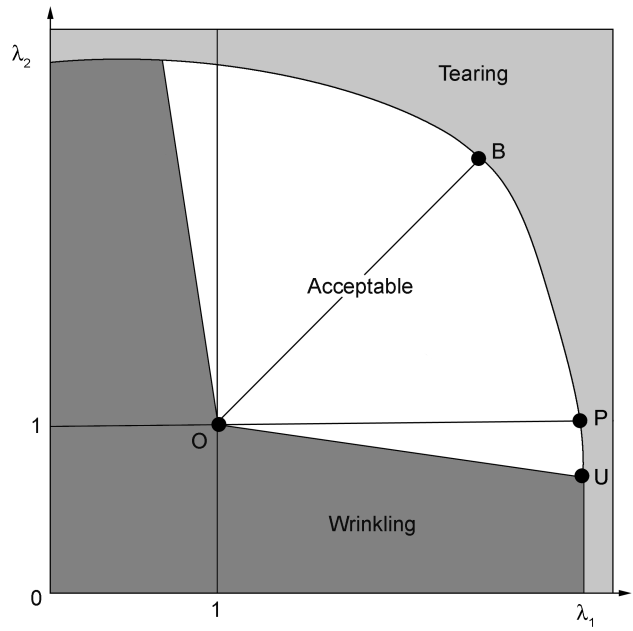

5.9 Qualitative forming limit diagram, showing regions of acceptable deformation, wrinkling, and tearing for random fiber mat (Tucker, 1998).

shape as well as other processing conditions. Both parameters should be optimized for high quality composite forming, and concurrent optimization may be possible using schemes set out in Equation (5.10), adding a shape parameter for preform shape, such as, for example, the coefficients of a parametric curve representing preform shape. However, a direct method for preform (prepreg) shape optimization can be effectively formulated. A separate scheme for optimizing both processing parameters is discussed in Sections 5.3.2 and 5.3.3.

5.3.2 Shape optimization using a direct method

The initial preform (blank) shape is known to determine the deformation behavior of preform in forming. In the metal forming field, researchers have performed many studies to design an initial blank shape with optimum deformation for a specific product shape (e.g., Chung, 1992a, 1992b, 1997). The basic aim of these studies is to define a path which produces a desired homogeneous deformation with minimum plastic work. It is also assumed in the studies that the formability of local material elements is optimum when they deform following a minimum work path. An ideal process is then defined as the one having local deformations that are optimally distributed in the final shape, through which an ideal initial configuration is determined to form a specified final shape.

In composite forming, the preform shape is also an important element in determining the deformation shape. Experimental observation representing the importance of the blank shape design was reported by O'Bradaigh (1997) who formed several specimens modified from a square blank (APC-2 carbon/PEEK) by cutting some corners and showed improved wrinkling behavior. By using a diaphragm forming process a significant and positive correlation was found between the shape of a blank and the wrinkling behaviour. Simulation results have also demonstrated the effect of preform shape on the forming behavior (Yu, 2005). As such, preform shape is an object to be optimized in the composite forming process. A method of optimally designing a blank is now discussed.

In composite forming, limited research has been conducted on the blank design for forming a specified product. One research study (Tucker, 2003) performed an ideal forming analysis for a random fiber reinforcement by utilizing the forming limit diagram. The researchers in this study determined a potential representing the formability of the reinforcement obtained by measuring the stretching behavior of the preform along several deformation paths and then by setting an upper forming limit as shown in Equation (5.11):

$$W = (\lambda_1 - 1)^2 + (\lambda_2 - 1)^2 + \frac{\alpha}{2}\mathbf{c} \cdot \mathbf{c} \qquad 5.11$$

where λ_1 and λ_2 are principal stretches, and α and $\mathbf{c}$ are penalty constant and a vector describing the forming limit in Fig. 5.9.

The first two terms on the right-hand side in Equation (5.11) keep the deformation state as close to the undeformed state as possible, assuming that defects are directly linked to the deformation. This assumption is only valid for composite preform because in sheet metal forming material needs to be stretched to impart work-hardened behavior. The third term in Equation (5.11) is a quadratic penalty function to enforce the forming limits of materials, which were obtained experimentally. The constraint vector $\mathbf{c}$ contains those constraints that are violated, while α is a non-negative penalty parameter controlling the strength with which the forming limits are enforced. The researchers determined a forming limit diagram for Vetrotex CertainTeed's U750 mat experimentally as shown in Fig. 5.10. The potential was then minimized to seek an initial blank shape based on the premise that an initial configuration is ideal if the deformation of all elements within the initial blank resides within the forming limit. The solution procedure for this method is explained briefly here following the works of Chung (1992a, 1992b, 1997) and Tucker (2003).

Consider that a final shape to be formed is characterized by a surface description, for example $x_3 = f(x_1, x_2)$. Optimization for the blank design can be summarized as a task of seeking an initial blank shape in terms of X_1 and X_2 if the initial configuration is assumed as a flat sheet (i.e., $X_3 = 0$). Alternatively, the final shape is conveniently described by a finite element mesh fixed in the global coordinates (x_1, x_2, x_3) using surface coordinates. For the finite element

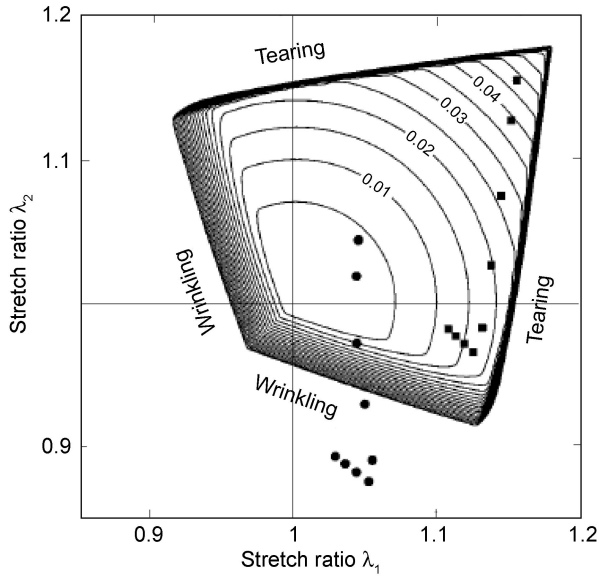

5.10 Contour plot of the formability function *W* for 750U random-fiber mat where $\alpha = 100$ (Tucker, 2003).

meshes given, the blank shape optimization process involves inversely calculating the initial coordinates of nodes of all elements in the final mesh. Note that the unknown variables are X_1 and X_2 (in the initial configuration), while general FE analysis aims to obtain x_1, x_2 and x_3 based on X_1 and X_2. A mapping function is introduced to calculate the initial configuration of the elements. The mapping function includes non-physical energy representing deviation from the forming limit, and can be expressed using the forming limit diagram formula set out in Equation (5.12) as follows:

$$\Pi = \int (W(\lambda_1, \lambda_2)) dV^0 \qquad 5.12$$

Equation (5.12) can be expressed with the final configuration using Jacobian between the initial and final configuration, as follows:

$$\Pi = \int \left(\tilde{W}(\lambda_1, \lambda_2)\right) dV \qquad 5.13$$

where $\tilde{W}(\lambda_1, \lambda_2) = \dfrac{1}{\lambda_1 \lambda_2} W(\lambda_1, \lambda_2)$.

The stretch is determined when the initial (X_1 and X_2) and final (x_1, x_2 and x_3) configurations are given. Since in this case the final shape is given, the stretch is a function of the initial coordinate. Since the mapping function represents a high value for a portion of the blank which falls on the outside of the forming limit, the optimization of the blank shape is mathematically equivalent to a

configuration that makes the mapping function minimum. The minimum of Equation (5.14) can be determined by requiring that the derivative of Π with respect to the initial sheet configuration be zero, as follows:

$$\frac{d\Pi}{d\mathbf{X}} = 0 \tag{5.14}$$

where $\mathbf{X} = (X_1, X_2)$. Numerical simulation is performed by discretizing Equation (5.13) using finite element approximation and by translating Equation (5.14) as an *n*-dimensional equation (where *n* equals the total number of nodal points in the final and initial mesh). The Newton-Raphson (NR) method is employed to find the initial coordinates of element nodes corresponding to the final one. Since the NR solution will converge only when a good initial guess for the solution variables is provided, it is critical to choose a proper initial guess. The easiest way for determining the initial shape is to project all the nodes on the final surface onto the X-Y plane. However, this may make it difficult to converge to a solution, particularly for deep curved structures. For the two fiber directional preform, such as a woven structure, a flat pattern can be obtained from the iterative energy minimization code (Long, 2002), which can be tried for the initial guess.

Figure 5.11 shows the final shape (box with flange preform) and the initial blank shape as optimized using the direct method. As shown in Fig. 5.11, large values of the formability function are observed in both the upper corner and in the adjacent flange area, indicating possible defects in these two regions. The optimal preform obtained in this work may not conform to the final shape in real forming because this simulation does not consider processing conditions such as the blank holding force and friction between tools and preform. Iterative simulation could be further performed to include these processing conditions, adjusting the initial blank shape to be more conformable to the final shape (Park, 1999). Recently, a new formulation considering the blank holding force and friction has been developed in the metal forming field and this can also be used in composite forming (Chung, 2000).

In this section, the shape optimization method, which does not rely on manual input to drive the successive iteration for optimization, is discussed. To employ this kind of optimization strategy for optimum blank design, a mapping function, which can be based on formability or deformation theory (Chung, 1993) for sheet metal, should be developed. For the continuous fiber preform, such a mapping function may be formulated based on fiber angle limit, wrinkling criterion, or fiber breakage.

5.3.3 Optimization of process parameters using iterative optimization method

In the previous section, the optimization of preform shape, one of the important process parameters, was discussed. Since other processing parameters are

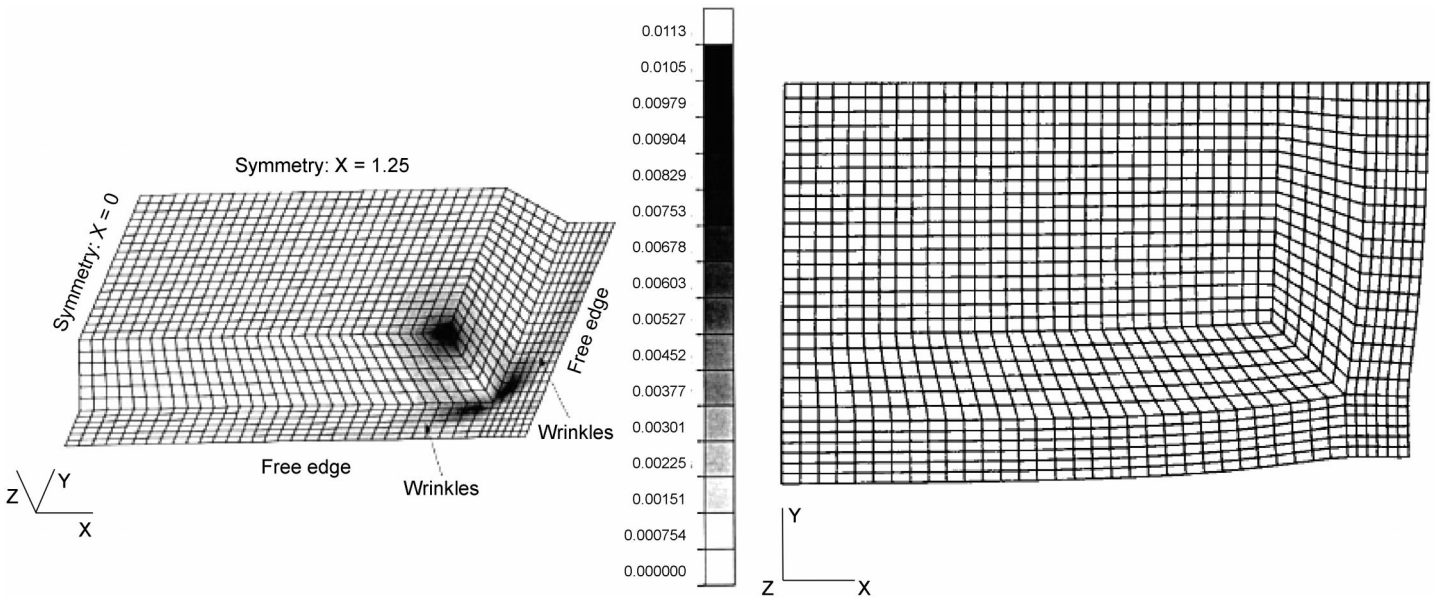

5.11 Target shape with contour plot of the formability function (left) and initial blank preform required to produce the optimal preform (right) for the target shape (Tucker, 2003).

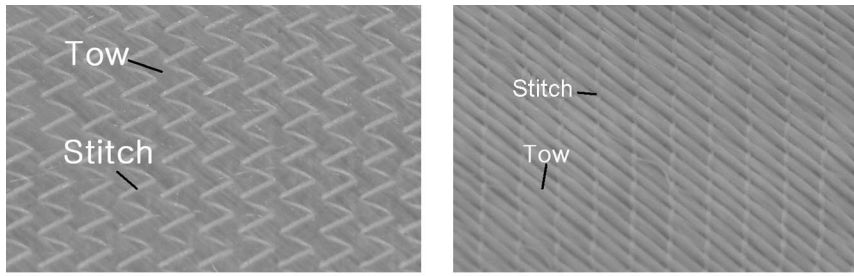

(a) Technical face (b) Technical back

5.12 Surface structure of an NCF with tricot stitch.

involved in composite forming besides preform shape, the quality of a formed product can be improved by properly choosing processing parameters. Among the many processing parameters, BHF is recognized as an important factor for composite preform because less tension causes wrinkling in the preform due to compressive stress, while too much tension can bring about fiber breakage. In contrast to the preform shape optimization process, BHF can be optimized using the iterative optimization method explained in Section 5.2. Through experimental observations, the effect of BHF on the forming behavior is first discussed.

The forming of non-crimp fabric (NCF) with tricot stitch is chosen as an example for investigating the effect of BHF on the formed shape (Lee, 2006). As shown in Fig. 5.12, the stitch pattern was introduced to hold the warp and weft yarn together in such fabric. Due to the stitch, the fiber angle between the warp and the weft in as-received NCF is a little deviated from 90º, the actual fiber angle measured being 97º.

Stitch pattern and fiber orientation are known to be crucial factors in determining the forming behavior of NCF. To address the effect of these two factors on forming behavior, two square samples of 350 mm × 350 mm in dimension were prepared cutting glass NCF using a die cutter; one sample (TC_N) with the warp and weft aligned parallel to the edge of a square; the other sample (TC_D) with the warp and the weft aligned in the diagonal of a square. On each sample four different axes (ST90, Warp, ST, Weft) were marked on which fiber angle and node displacement were measured at every 15mm interval in order to quantify the deformation behavior of NCF. Note that the ST90 and ST axes are referred to the directions perpendicular and parallel to the stitches respectively. A hemispherical forming system was designed that is attachable to a laboratory UTM (Universal Testing Machine-MTS). Figure 5.13 shows the schematic diagram of the hemispherical forming station employed in this discussion. The radius of the hemisphere punch was 75 mm, and the area of the blank holder was 0.017 m^2.

The punch stamps NCF into a hemispherical shape with a depth of 75 mm during one minute. Then, the formed NCF was hardened for 30 minutes using

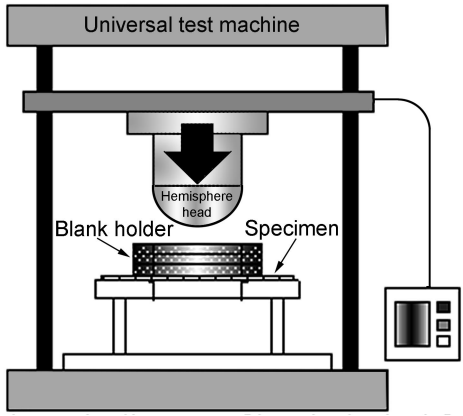

5.13 Schematic diagram of hemispherical forming process.

unsaturated polyester resin. The NCF was removed from the mold in order to measure and characterize the formed shape. The local fiber angle change of the formed NCF was measured by a goniometer, while node displacement was recorded through spatial coordinates obtained using a three-dimensional digitizer. The formed shape of NCF was quantified by measuring the shear angle and arc length along four different axes of the formed NCF. For this forming experiment, 19.4 kg of BHF was applied to both TC_D and TC_N samples. Fiber angles on the warp and weft axes were rarely changed while they were changed considerably on the ST90 and ST directions because compliance to shear deformation in these directions was relatively large. Note that the fiber angle change of ST90 axis was about 30º around the equator where maximum shear deformation was developed while 20º of fiber angle change was observed in the ST direction (see Fig. 5.14). Such an asymmetric shear angle pattern might be caused by stitches because, as observed in the picture-frame shear test (Long, 2002), the stitch structure determines shear resistance according to shear direction.

It is interesting to note that the shear angle of ST and ST90 in TC_N was larger than one of the same direction in the TC_D sample, while the fiber angle in the fiber direction of both samples was little changed. This result clearly shows the effect of blank shape on the forming behavior. If both samples had been prepared in a circular blank shape, the fiber angle changes would have been the same because the fiber orientation and stitches in them were the same. Since a square blank shape was used in this experiment, the excess part of the square had a different fiber orientation; fibers in the TC_N sample were aligned in a ±45º direction based on the square diagonal while fibers in the TC_D sample were aligned diagonally, making the shearing more difficult in the TC_D sample.

Figure 5.15 shows the formed shapes of NCF samples (TC_N and TC_D) according to BHF. Two noticeable features of the BHF effect can be observed in

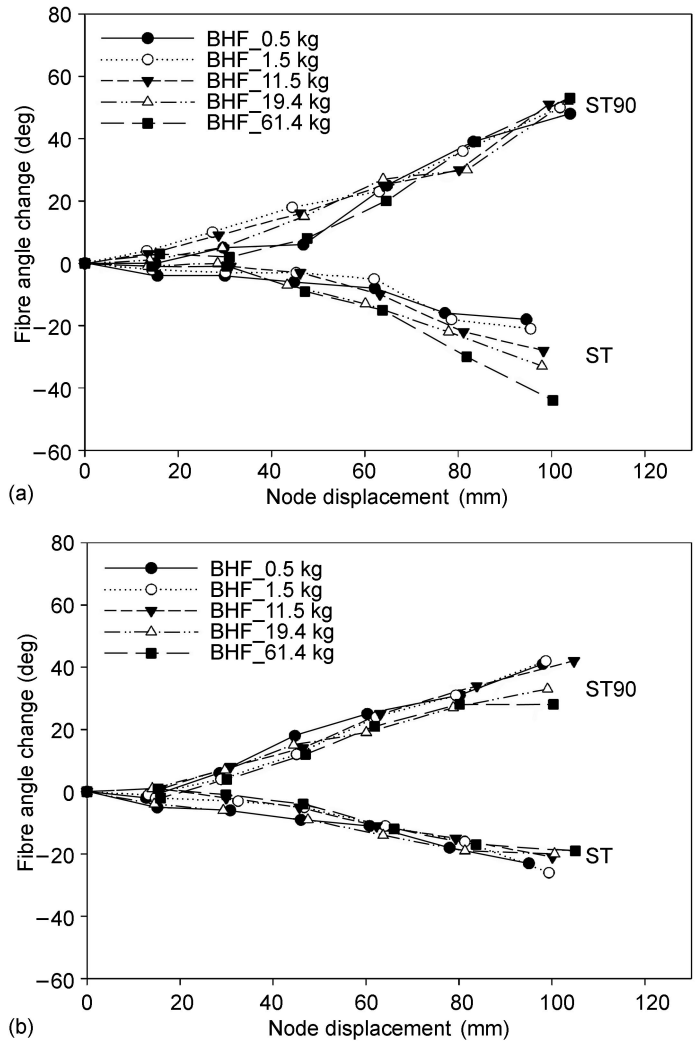

5.14 Fiber angle change in the ST90 and ST directions according to BHF (a) TC_N and (b) TC_D.

both sample cases. For small BHF ((a) and (c) in Fig. 5.15), both samples (TC_N and TC_D) were formed into a hemispherical shape with severe asymmetric deformation and wrinkling around the equator. This was due to insufficient tension applied to the NCFs during forming, in which compression stress was developed in a circumferential direction. As BHF increased, the formed shape changed dramatically into the symmetrical formed shape. From the experiments, it may be concluded first that BHF is a very important factor in determining the forming behavior of NCF and secondly that optimization of BHF may enable a

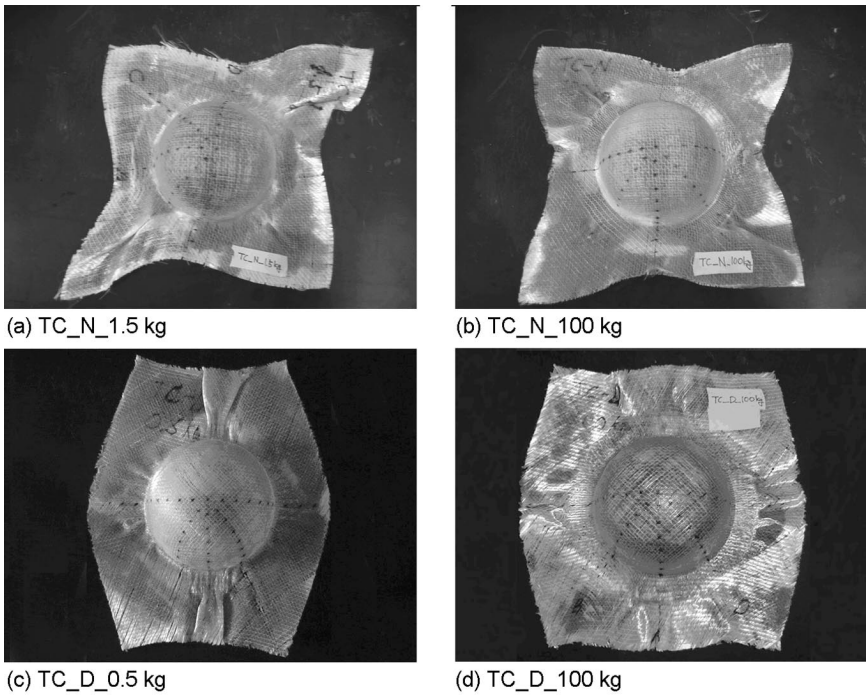

5.15 Formed shapes of NCF (TC_N and TC_D samples).

significant reduction in wrinkling. Wrinkle and in-plane buckling were observed near the equator in the warp and weft fiber direction axes. To clearly investigate wrinkling with high frequency and small magnitude, a slit laser shed light on the surface of the formed sample. As shown in Fig. 5.16, the laser light was more scattered around the equator of a hemispherical formed NCF where the wrinkles were propagated severely. Note that for a region without wrinkles, or with fewer wrinkles, the laser was more visible in a straight line. As BHF increased in the

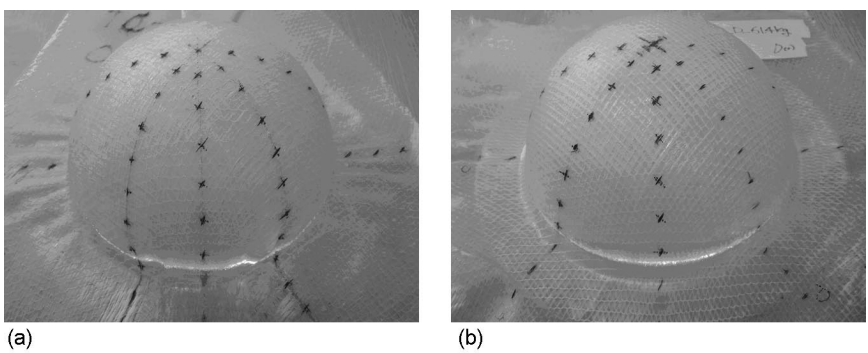

5.16 Wrinkling visualization of formed NCF (TC_D sample).

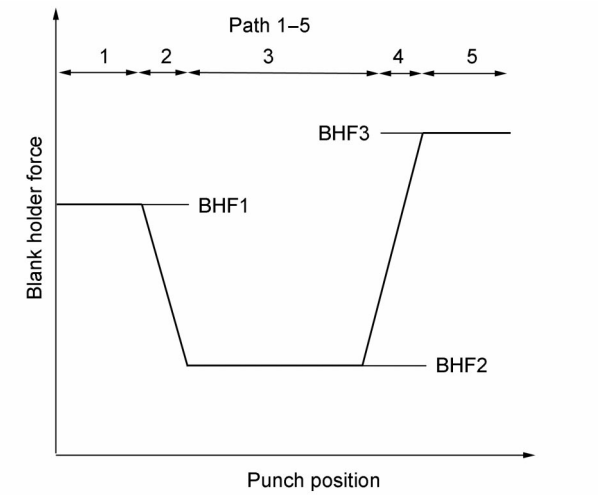

5.17 Figure blank holder force as a function of the drawing depth described by seven parameters (Jakumeit, 2005).

forming operation, laser scattering was reduced which indicated a reduction in wrinkling. With this experiment, it can be confirmed that wrinkling in the formed NCF can be reduced through the optimization of BHF.

As discussed so far, the blank holder force is a crucial factor in determining the forming behavior of composite preform. Optimization of the blank holding force can be performed based on experiments, but systematic optimization of

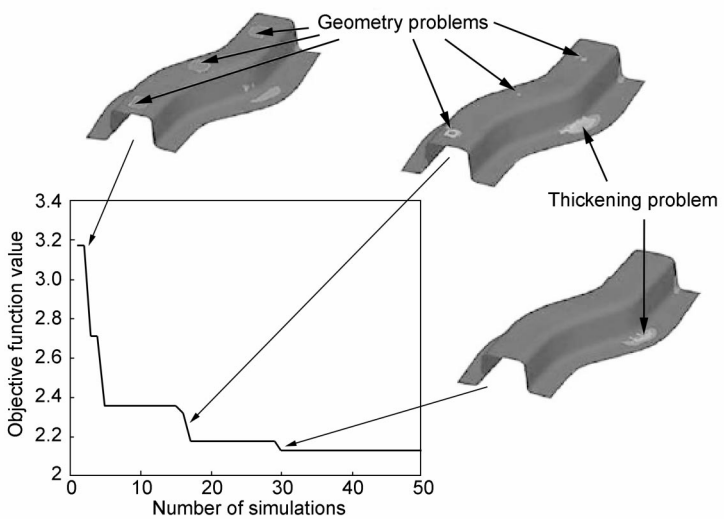

5.18 Convergence behavior of the Kriging strategy for the SRAIL test of a metal sheet (Jakumeit, 2005).

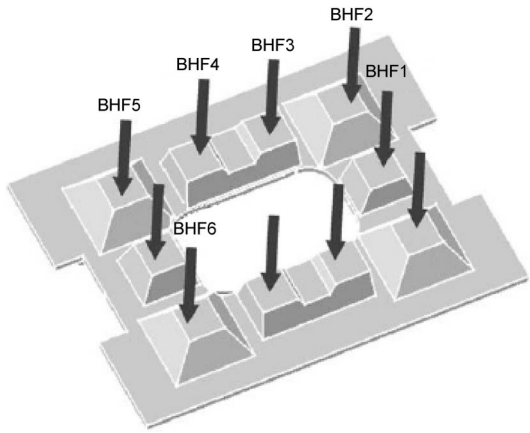

5.19 The schematic diagram of the segmented blank holder (Chengzhi, 2005).

BHF may need to include a variable BHF (Fig. 5.17) and segmented blank holder (Fig. 5.19) whereby numerical simulations or computational experiments are inevitable for including various ranges of blank holding force profiles. In the sheet metal forming field in which the formability function (objective function)

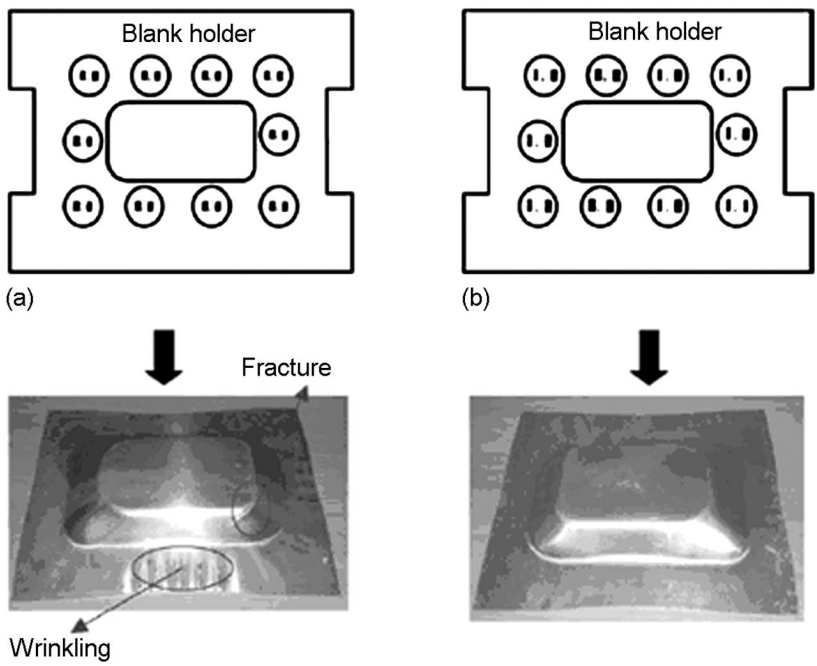

5.20 Stamped sheet metal under initial BHFs (left) and optimal BHFs (right) (Chengzhi, 2005).

was well defined, the optimization of blank holding force has been endeavored to minimize an objective function, which was constructed based on the formability function, using the iterative algorithm described in the previous section. Figures 5.18 and 5.20 demonstrate how well formed parts can be improved by controlling BHF. Since the formability of composite preform has been less established, future study for composite forming optimization should be dedicated to developing an objective function that takes into account fiber angle.

5.4 Conclusions

In this chapter, optimization for composite forming was discussed with objective functions which are essential elements in forming optimization. Among processing parameters in the composite forming process, preform (blank shape) and BHF were identified as essential quantities which should be optimized for better quality of formed preform. Actual methods for optimization were discussed, which can be classified in terms of direct and indirect (iterative) methods. The direct method is to formulate an objective function through a finite approximation of an initial and final blank, and to calculate inversely the initial configuration of preform corresponding to the final one, thereby excluding successive manual inputs to drive an optimization iteration. Though the direct method can save design time because it is not based on trial-and-error practices, it cannot consider actual processing parameters, such as the variable BHF. Indirect (or iterative) methods can be applied to the optimization of processing parameters, though such methods need manual input to drive successive iterations in the optimization process, necessitating an optimization method that can utilize parallel simulations. For the successful implementation of both methods, objective functions should be established that assess the quality of formed parts in terms of processing parameters, and future research should be focused in this direction for the optimization of composite forming.

5.5 References

Chengzhi S, Guanlong C, Zhongqin L (2005), 'Determining the optimum variable blankholder forces using adaptive response surface methodology (ARSM)', *Int J Adv Manuf Technol*, 26, 23–29.

Chung K, Richmond O (1992a), 'Ideal forming-I. Homogeneous deformation with minimum plastic work', *Int J Mech Sci*, 34(7), 575–591.

Chung K, Richmond O (1992b), 'Ideal forming-II. Sheet forming with optimum deformation', *Int J Mech Sci*, 34(8), 617–633.

Chung K, Richmond O (1993), 'A deformation theory of plasticity based on minimum work paths', *Int J Plast*, 9, 907–920.

Chung K, Barlat F, Brem J C, Lege D J, Richmond O (1997), 'Blank shape design for a planar anisotropic sheet based on ideal forming design theory and FEM analysis', *Int J Mech Sci*, 39(1), 105–120.

Chung K, Yoon J W, Richmond O (2000), 'Ideal sheet forming with frictional constraints', *Int J Plast*, 16, 595–610.

Delaloye S, Niedermeier M (1995), 'Optimization of the diaphragm forming process for continuous fiber-reinforced advanced thermoplastic composites', *Compos Manuf*, 6, 135–144.

Hou M, Friedrich K, Scherer R (1994), 'Optimization of stamp forming of thermoplastic composite bends', *Compos Struct*, 27, 154–167.

Jakumeit J, Herdy M, Nitsche M (2005), 'Parameter optimization of the sheet metal forming process using an iterative parallel Kriging algorithm', *Struct Multidisc Optim*, 29, 488–507.

Lee J S, Hong S J, Yu W-R, Kang T J (2006), 'The effect of blank holding force on the stamp forming behavior of non-crimp fabric with a chain stitch', *Compos Sci Technol*, in press.

Long A C, Souter B J, Robitaille F, Rudd C D (2002), 'Effects of fibre architecture on reinforcement fabric deformation', *Plast Rubber Compos*, 31(2), 87–97.

Lophaven S N, Nielsen H B, Sondergaard J (2002), http://www2.imm.dtu.dk/~hbn/dace/.

Luenberger D G (1989), *Linear and Nonlinear Programming*, Massachusetts, Addison-Wesley.

Myers R H, Montgomery D C (2002), *Response Surface Methodology*, New York, John Wiley & Sons.

O'Bradaigh C M, McGuinness G B, McEntee S P (1997). 'Implicit finite element modelling of composites sheet forming processes' in Bhattacharyya D, *Composite Sheet Forming*, Amsterdam, Elsevier, 247–322.

Park S H, Yoon J W, Yang D Y, Kim Y H (1999), 'Optimum blank design in sheet metal forming by the deformation path iteration method', *Int J Mech Sci*, 41, 1217–1232.

Press, W H, Teukolsky, S A, Vetterling W T, Flannery B P (1992), *Numerical Recipes in C*, Cambridge, Cambridge University Press.

Prodromou A G, Chen J (1997), 'On the relationship between shear angle and wrinkling of textile composite preforms', *Compos Part A-Appl S*, 28A, 491–503.

Sacks J, Welch W J, Mitchell T J, Wynn H P (1989), 'Design and analysis of computer experiments', *Statistical Science*, 4(4), 409–435.

Tucker C L, Dessenberger R B (1998), 'Forming limit measurements for random-fiber mat', *Polym Composite*, 19(4), 370–376

Tucker C L, Dessenberger R B (2003), 'Ideal forming analysis for random fiber preforms', *J MANUF SCI E-T ASME*, 125, 146–153.

Yu W R, Pourboghrat F, Chung K, Zampaloni M, Kang T J (2002), 'Non-orthogonal constitutive equation for woven fabric reinforced composites', *Compos Part A-Appl S*, 33, 1095–1105.

Yu W R, Harrison P, Long A (2005), 'Finite element forming simulation for non-crimp fabrics using a non-orthogonal constitutive equation', *Compos Part A-Appl S*, 36, 1079–1093.